Re-ranking via Local Embeddings: A Use Case with Permutation-based Indexing and the nSimplex Projection ☆

Lucia Vadicamo[a,*], Claudio Gennaro[a], Fabrizio Falchi[a], Edgar Chávez[b], Richard Connor[a], Giuseppe Amato[a]

[a] *Institute of Information Science and Technologies (ISTI), CNR, Pisa, Italy*
[b] *Centro de Investigación Científica y de Educación Superior de Ensenada (CICESE), Ensenada, Mexico*

Abstract

Approximate Nearest Neighbor (ANN) search is a prevalent paradigm for searching intrinsically high dimensional objects in large-scale data sets. Recently, the permutation-based approach for ANN has attracted a lot of interest due to its versatility in being used in the more general class of metric spaces. In this approach, the entire database is ranked by a permutation distance to the query. Typically, permutations allow the efficient selection of a candidate set of results, but typically to achieve high recall or precision this set has to be reviewed using the original metric and data. This can lead to a sizeable percentage of the database being recalled, along with many expensive distance calculations.

To reduce the number of metric computations and the number of database elements accessed, we propose here a re-ranking based on a local embedding using the nSimplex projection. The nSimplex projection produces Euclidean vectors from objects in metric spaces which possess the n-point property. The mapping is obtained from the distances to a set of reference objects, and the original metric can be lower bounded and upper bounded by the Euclidean distance of objects sharing the same set of references.

Our approach is particularly advantageous for extensive databases or expensive metric function. We reuse the distances computed in the permutations in the first stage, and hence the memory footprint of the index is not increased.

An extensive experimental evaluation of our approach is presented, demonstrating excellent results even on a set of hundreds of millions of objects.

Keywords: metric search, permutation-based indexing, n-point property, nSimplex projection, metric local embeddings, distance bounds

* Corresponding author

Email addresses: `lucia.vadicamo@isti.cnr.it` (Lucia Vadicamo), `claudio.gennaro@isti.cnr.it` (Claudio Gennaro), `fabrizio.falchi@isti.cnr.it` (Fabrizio Falchi), `elchavez@cicese.mx` (Edgar Chávez), `richard.connor@isti.cnr.it` (Richard Connor), `giuseppe.amato@isti.cnr.it` (Giuseppe Amato)

1. Introduction

Proximity search is successfully used to retrieve data objects that are close to a given query object under some metric function. It has a vast number of applications in many branches of computer science, including pattern recognition, computational biology, and multimedia information retrieval, to name but a few. This search paradigm, referred to as *metric search*, is based on the assumption that data objects are represented as elements of a metric space (D, d) where the *metric*[1] function $d : D \times D \rightarrow \mathbb{R}^+$ provides a measure of the closeness of the data objects.

In metric search algorithms, the main concern is processing and structuring a finite set of data $X \subset D$ so that *proximity queries* can be answered quickly and with a low computational cost. A proximity query is defined by a query object $q \in D$ and a proximity condition, such as "find all the objects within a threshold distance of q" (*range query*) or "finding the k closest objects to q" (*k-nearest neighbour query*). The response to a query is the set of all the objects $o \in X$ that satisfy the considered proximity condition. In this work, we focus on the k-nearest neighbour (k-NN) search since, as also highlighted in [2, 3], (i) it allows us to control the size of the results set, and (ii) it is simpler to use in high-dimensional space where it is not obvious to define a meaningful distance value to be used with other search paradigms, like the range query. However, providing an exact response to a k-NN query is not feasible if the search space is very large or it has a high intrinsic dimensionality since it would be necessary to inspect a large fraction of the data to process the query. In such cases, the exact search rarely outperforms a sequential scan [4, 5]. To overcome this phenomenon, known as *curse of dimensionality* [6], researchers proposed several *approximate search* methods that are less (but still) affected by it. The main idea of approximate methods is to efficiently find a set of results that is likely to contain most of the objects that satisfy the query proximity condition. However, the efficiency of these methods comes at the expense of a certain reduction of the accuracy (e.g. false hits or missing results). A limited imprecision in the response to the query, however, is tolerable in many applications, such as multimedia retrieval where the concept of "(dis)similarity" may differ according to user expectations, and close approximations may be good enough for human perception [7].

Many Approximate Nearest Neighbor (ANN) methods are based on the idea of mapping the data objects into a more tractable space in which we can efficiently perform the search. Successful examples are the *Permutation-Based Indexing* (PBI) approaches that represent data objects as a sequence of identifiers (*permutation*). Typically, the permutation for an object o is computed as a ranking list of some preselected reference points (*pivots*) according to their distance to o. The main rationale behind this approach is that if two objects are very close one to the other they will sort the set of pivots in a very similar way, and thus the corresponding permutation representations will be close as well. The search in the permutation space is used to select a candidate result set that is then typically refined by comparing each element of the candidate set to the query, according to the metric governing the original data space. This refinement step, therefore, requires access to the original data, which is likely to be too large to fit into the main memory. However, some kind of refinement step is likely to be necessary as the search in the permutation space usually has relatively low precision.

In this paper, we focus on permutation-based k-NN search and we investigate several approaches to perform the refining step without access to the original data. Our techniques approximate the actual distance between a query and the candidate objects by exploiting the distances

[1] Throughout this paper, we use the terms "metric" and "distance" interchangeably to indicate a function satisfying the metric postulates of non-negativity, identity, symmetry, and triangle inequality [1].

Table 1: Notation used throughout this paper

Symbol	Definition
(D, d)	metric space
X	finite search space, $X \subseteq D$
$\mathcal{P}_n = \{p_1, \ldots, p_n\}$	set of pivots, $p_i \in D$
n	number of pivots
o, s	data objects, $o, s \in X$
q	query, $q \in D$
k, k'	number of results of a nearest neighbour search
Π_o	pivot permutation
Π_o^{-1}	inverted permutation
l	permutation prefix length (location parameter)
$\Pi_{o,l}$	permutation prefix of length l (truncated permutation)
$\Pi_{o,l}^{-1}$	inverted truncated permutation
$PivotSet(\Pi_{o,l})$	the pivots whose identifiers appear in $\Pi_{o,l}$
$\Gamma_{o,q}$	pivots in the intersection $PivotSet(\Pi_{q,l}) \cap PivotSet(\Pi_{o,l})$
$S_{\rho,l}$	Spearman's rho with location parameter l
ℓ_2	Euclidean distance
ℓ_∞	Chebyshev distance
$f_{\mathcal{P}_n} : (D, d) \rightarrow (\mathbb{R}^n, \ell_\infty)$	Pivoted embedding
$\phi_{\mathcal{P}_n} : (D, d) \rightarrow (\mathbb{R}^n, \ell_2)$	nSimplex projection
$\lvert \cdot \rvert$	size of a set

between the objects and the pivots (calculated at indexing time and stored within the permutations) and the distances between the query and the pivots (evaluated when computing the query permutation). In particular, for a large class of metric spaces that meet the so-called "*n-point property*" [8, 9] we propose the use of the *nSimplex projection* [10] that allows mapping metric objects into a finite-dimensional Euclidean space where upper- and lower- bounds for the original distances can be calculated. We show how these distance bounds can be used to improve the permutation-based results without accessing to the original data set.

A preliminary version of this work appeared in [11]. The present contribution gives, also, a more detailed description of the proposed approaches and an extensive experimental evaluation. In particular, it includes new results on large scale and investigates the use of compressed versions of the inverted files to index the data. The rest of the paper is structured as follows. Section 2 reviews related work. Section 3 provides basic concepts of the metric space transformations used in our work (namely, permutation-based representations, Pivoted embedding, and nSimplex projection). In Section 4 we describe several pivot-based approaches to refine a permutation-based candidate set. A detailed experimental evaluation and analysis of those approaches is presented in Section 5. Finally, the conclusions are drawn in the last section.

Table 1 summarises the notation used in this paper.

2. Related Work

The idea of approximating the distance between any two metric objects by comparing their permutation-based representations was originally proposed in [12, 13]. Several techniques for indexing and searching permutations were considered in literature, including indexes based on inverted files, like the *Metric Inverted File* (MI-File) [14] and its variants [15], or using prefix trees, like the *Permutation Prefix Index* (PP-Index) [2] and the *Pivot Permutation Prefix Index* (PPP-Index) [16]. In [17], the metric objects in the inverted index are represented by a signature built from the l nearest references to them. However, in all above approaches, the candidate result set identified by performing the search in the permutation space should be refined to achieve high effectiveness. Typically the results are refined by directly comparing the query object with the candidate results obtained according to the original distance and data representation.

The common approach to generate a permutation-based representation of a data object is to sort the identifiers of a set of pivots according to their distances to the object [18]. However, the computation of these distances is just one, yet effective, approach to associate a permutation to each data object. For example, the *Deep Permutations* [19] have recently been proposed as an efficient and effective alternative for generating permutations of emerging deep features. Nevertheless, this approach is only suitable for specific data domains whereas the traditional approach is generally applicable as it requires only the existence of a distance function to compare data objects.

In [20], Figueroa et al. have tried different distances between permutations instead of the canonical Spearman's Footrule or Spearman's rho metrics. The aim of this work, however, was to reduce the number of distance computations and the size of the index.

The distances between the data objects and a set of pivots can also be used to embed the data into another metric space where upper and lower bounds of the actual distance between any pair of objects can be calculated. In this context, one of the very first embeddings proposed in a metric search scenario was the one representing each data object with a vector of its distances to the pivots. The LAESA [21] is a notable example of indexing technique using this approach. Connor et al. [10, 9, 22] observed that for a large class of metric spaces it is possible to use the distances from a set of n pivots to project the data objects into a n-dimensional Euclidean space so that in the projected space 1) the distances object-pivots are preserved, 2) the Euclidean distance between any two points is a lower-bound of the actual distance, 3) also an upper-bound can be easily computed. They called this approach *nSimplex projection* and they proved that it can be used in all the metric spaces meeting the *n-point property* [23]. As also pointed out in [8], many common metric spaces meet the desired property, like Cartesian spaces of any dimension with the Euclidean, Cosine or Quadratic Form distances, probability spaces with the Jensen-Shannon or the Triangular distances, and more generally any Hilbert-embeddable space [23, 24].

Recently, the nSimplex projection has been exploited to generate a novel permutation-based representation for metric objects, called SPLX-Perm [25]. It is based on the idea of mapping the data object to Euclidean vectors, which are in turn transformed into permutations using an approach similar to that used in the Deep Permutations [19].

3. Background

Many metric space transformations proposed in the literature were designed with the aim of mapping the original data to a space that has better indexing properties than the original one, or where the function used to compare the objects is less expensive than the original distance. In this

section, we summarise key concepts of some metric transformations that exploit the distances between data objects and a set of pivots for projecting the data. In particular, we review data transformations into permutation spaces (where objects can be efficiently indexed using PBI methods) and two pivot-based embeddings that allow computing upper- and lower- bounds of the actual distance.

3.1. Permutation-Based Representations

Let $\mathcal{D}$ a data domain, $d : \mathcal{D} \times \mathcal{D} \rightarrow \mathbb{R}^+$ a *metric* function on it[2], and $\mathcal{P}_n = \{p_1, \ldots, p_n\} \subset \mathcal{D}$ a fixed set of *pivots*. A permutation-based representation Π_o (briefly *permutation*) of an object $o \in \mathcal{D}$ with respect to the pivot set $\mathcal{P}_n$ is the sequence of the pivots identifiers ordered by their distance to o.

Formally, the permutation $\Pi_o = [\Pi_o(1), \Pi_o(2), ..., \Pi_o(n)]$ lists the pivot identifiers $\{1, \ldots, n\}$ in an order such that $\forall\, i \in \{1, \ldots, n-1\}$,

$$d(o, p_{\Pi_o(i)}) < d(o, p_{\Pi_o(i+1)}) \tag{1}$$

or

$$\left[d(o, p_{\Pi_o(i)}) = d(o, p_{\Pi_o(i+1)})\right] \wedge \left[\Pi_o(i) < \Pi_o(i+1)\right]. \tag{2}$$

Several PBI methods, such as [2, 14, 16], do not use the full-length permutation to represent a data object o, but instead use a fixed-length prefix of it, i.e. $\Pi_{o,l} = [\Pi_o(1), \ldots, \Pi_o(l)]$, which is called *permutation prefix* or *truncated permutation of lenght l*. This choice is based on the intuition that the most relevant information in the permutation is present in its very first elements, i.e. the identifiers of the closest pivots. Moreover, using the positions of the nearest l out of n pivots often leads to obtaining better or similar effectiveness then using the full-length permutation [14, 18], resulting also in a more compact data encoding.

Several metric functions have been used in literature to compare permutations. Notable examples are Kendall's tau, Spearman's rho and the Spearman's Footrule distances. The permutation prefixes are usually compared using *top-l distances* [26], such as the Spearman's rho with location parameter l. It is worth noting that most of the commonly-used distances between (truncated) permutations can be easily computed as distances between Cartesian points by using the so called *inverted (truncated) permutations*.

The *inverted permutation* of $o \in \mathcal{D}$ is defined as $\Pi_o^{-1} = [\Pi_o^{-1}(1), \ldots, \Pi_o^{-1}(n)]$, where $\Pi_o^{-1}(i)$ denotes the position of a pivot p_i in the permutation Π_o. The inverted permutation is such that $\Pi_o(\Pi_o^{-1}(i)) = i$. Note that the value at the coordinate i in the permutation Π_o is the identifier of the pivot at i-th position in the ranked list of the nearest pivots to o; the value at the coordinate i in the inverted representation Π_o^{-1} is the rank of the pivot p_i in the list of the nearest pivots to o. The *inverted truncated permutation* $\Pi_{o,l}^{-1}$ is computed as

$$\Pi_{o,l}^{-1}(i) = \begin{cases} \Pi_o^{-1}(i) & \text{if} \quad \Pi_o^{-1}(i) \leq l \\ l+1 & \text{otherwise} \end{cases} \tag{3}$$

In this work, we use the Spearman's rho (S_ρ) and the Spearman's rho with location parameter l ($S_{\rho,l}$) metrics to compare permutations and truncated permutation, respectively. By using the

[2]In this work, we focus on metric search. The requirement that the function d satisfies the metric postulates is sufficient, but not necessary, to produce a permutation-based representation. For example, d may be a dissimilarity function.

inverted permutation representations we can easily compute these distances as the Euclidean distances between two vectors:

$$S_\rho(\Pi_o, \Pi_s) = \ell_2(\Pi_o^{-1}, \Pi_s^{-1}) \tag{4}$$

$$S_{\rho,l}(\Pi_o, \Pi_s) = \ell_2(\Pi_{o,l}^{-1}, \Pi_{s,l}^{-1}). \tag{5}$$

for any two permutations Π_o, Π_s and for any prefix length l. Note that if $l = n$ then $S_{\rho,l}(\Pi_o, \Pi_s) = S_\rho(\Pi_o, \Pi_s)$.

3.2. Pivoted Embedding

Given a metric space (D, d) and a fixed set of pivots $\mathcal{P}_n = \{p_1, \ldots, p_n\}$, we can use the information provided by measuring the distances between each metric object and each pivot to embed the metric space into $(\mathbb{R}^n, \ell_\infty)$:

$$\begin{aligned} f_{\mathcal{P}_n} : (D, d) &\rightarrow (\mathbb{R}^n, \ell_\infty) \\ o &\rightarrow [d(o, p_1), \ldots, d(o, p_n)]\,. \end{aligned}$$

This space transformation, referred to as as *Pivoted embedding* in the following, allows us to easily compute upper-bound and lower-bound of the actual distances. In facts, the triangle inequality of the metric governing the space guarantees that

$$\max_{i=1,\ldots,n} |d(o, p_i) - d(s, p_i)| \leq d(o, s) \leq \min_{i=1,\ldots,n} |d(o, p_i) + d(s, p_i)| \tag{6}$$

which it means that $\ell_\infty(f_{\mathcal{P}_n}(o), f_{\mathcal{P}_n}(s))$ is a lower-bound of $d(o, s)$ and that also an upper-bound can be defined using the projected objects $f_{\mathcal{P}_n}(o)$, $f_{\mathcal{P}_n}(s)$ (see [1, pp.28]). Please note that if we use just a subset $\mathcal{P}_l$ of size l of the pivots $\{p_1, \ldots, p_n\}$, the corresponding mapping $f_{\mathcal{P}_l}$ provides upper- and lower- bounds that are less tight than that obtained using $f_{\mathcal{P}_n}$.

The Pivoted embedding is typically used in indexing tables like LAESA [21] or for space pruning [1]. However, in this work we do not use this space transformation for indexing purposes, but rather as a technique to approximate the distances between a query and data objects already indexed using a permutation-based approach (see also Section 4).

3.3. nSimplex Projection

The *nSimplex projection* [10] is a space transformation of the form

$$\phi_{\mathcal{P}_n} : (D, d) \rightarrow (\mathbb{R}^n, \ell_2)$$

that uses the distances to a set of pivots $\mathcal{P}_n = \{p_1, \ldots, p_n\}$ for embedding metric objects into a finite-dimensional Euclidean space. It can be applied to any metric space that satisfies the so called *n-point property* [23], which provides geometric guarantees stronger than the triangle inequality. In particular, a metric space has the n-point property if, and only if, any set of n points of the space can be *isometrically* embedded into a $(n-1)$-dimensional Euclidean space, i.e. there exists a mapping of those points to n Euclidean vectors that preserves all the $\binom{n}{2}$ inter-points distances. In other words, the n points can be isometrically mapped to the vertices of a $(n-1)$-dimensional simplex[3].

[3] A simplex is a generalization of a triangle (2-dimensional simplex) or a tetrahedron (3-dimensional simplex) in arbitrary dimensions. Specifically, the $(n-1)$-dimensional simplex generated by the vertices $v_1, \ldots, v_n$ equals the union of all the line segments joining v_n to the points of the $(n-2)$-dimensional simplex of vertices $v_1, \ldots, v_{n-1}$.

The n-point property guarantees that given the pivots $\{p_1, \ldots, p_n\}$, we can determine the vectors $v_{p_1}, \ldots, v_{p_n}$ such that

$$\forall\, i, j \in \{1, \ldots, n\} : \quad \ell_2(v_{p_i}, v_{p_j}) = d(p_i, p_j).$$

We refer the $(n-1)$-dimensional simplex generated by those vectors to as the *simplex base*. Then, for any further object $o \in D$ the $(n+1)$-point property guarantees that there exists a vertex $v_o \in \mathbb{R}^n$ such that

$$\forall\, i \in \{1, \ldots, n\} : \quad \ell_2(v_{p_i}, v_o) = d(p_i, o),$$

i.e., the vector v_o is the apex of a n-dimensional simplex built upon the simplex base where the length of the i-th edge connecting v_o to the simplex base equals the actual distance $d(p_i, o)$. The nSimplex projection $\phi_{\mathcal{P}_n}$ is the transformation that maps an object $o \in D$ to the apex $v_o \in \mathbb{R}^n$ built upon the simplex base. Connor et al. [10] provided an iterative algorithm to compute the coordinates of the vertices v_{p_i} of the simplex base as well as the coordinates of the apex v_o associated to a metric object o. Remark that this algorithm determines those coordinates by only exploiting the distances $d(p_i, p_j)$ and $d(p_i, o)$, for $i, j \in \{1, \ldots, n\}$. Moreover, the simplex base is computed once and is reused for projecting every data object. Given the distances $d(p_i, o)$, the cost for computing v_o is $O(n)$ Euclidean distances between vectors having less than n dimensions.

One of the main profitable aspects of the nSimplex projection is that in the transformed space we can easily compute upper- and lower-bounds of the actual distance between any two metric objects. In facts, for any two objects $o, s \in D$, given the projected vectors

$$\begin{aligned} \phi_{\mathcal{P}_n}(o) &= [x_1, x_2, \ldots, x_{n-1}, x_n] \\ \phi_{\mathcal{P}_n}(s) &= [y_1, y_2, \ldots, y_{n-1}, y_n] \end{aligned}$$

it holds

$$\sqrt{\sum_{i=1}^{n}(x_i - y_i)^2} \quad \leq \quad d(o, s) \quad \leq \quad \sqrt{\sum_{i=1}^{n-1}(x_i - y_i)^2 + (x_n + y_n)^2}. \tag{7}$$

Therefore, $\ell_2(\phi_{\mathcal{P}_n}(o), \phi_{\mathcal{P}_n}(s))$ is a lower-bound for $d(o, s)$. Moreover, if we consider the vector $\phi^-_{\mathcal{P}_n}(s) = [y_1, y_2, \ldots, y_{n-1}, -y_n]$ we have that an upper-bound for $d(o, s)$ can be computed as the the Euclidean distance between $\phi_{\mathcal{P}_n}(o)$ and $\phi^-_{\mathcal{P}_n}(s)$, i.e. $\ell_2(\phi_{\mathcal{P}_n}(o), \phi^-_{\mathcal{P}_n}(s))$. Interestingly, in [27, 10] it was shown that the nSimplex bounds become tighter with increasing number of pivots n.

Note that, as observed in [8, 10], there is a large class of metric spaces that satisfy the n-point property and therefore can be transformed by the nSimplex projection. Examples are given by the Euclidean spaces of any dimension, spaces with the Triangular or Jensen-Shannon distances, and, more generally, any Hilbert-embeddable spaces. Moreover, if a metric space does not meet the n-point property, (e.g. Hamming or Chebyshev metrics), there always exists a proximity preserving mapping of this space into a metric space with this property [28].

4. Re-ranking the Permutation-Based Candidate Set

The permutation-based methods for approximate search are filter-and-refine techniques that rely on the idea of transforming a metric space (D, d) into a permutation space. At query time, a set of candidate results for a given query $q \in D$ is obtained by performing a similarity search in the permutation space. The candidate results are then refined, typically by using the actual distance d to compare the candidate objects with the query one. Nevertheless, the refining approach

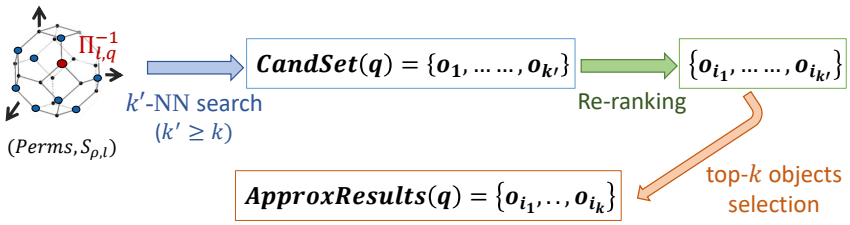

Figure 1: Illustration of the pipeline adopted in this work to compute the approximate k-NN results to a query by re-ranking a permutation-based candidate result set.

based on the actual distance requires to store the original data set and access to it at query time. Below, we investigate alternative refining approaches that do not require to access original data objects. The main objective is to improve the permutation-based results while getting rid of the original data set.

We focus on the k-NN search and we assume that a set of candidate results $CandSet(q)$, with $|CandSet(q)| = k' > k$, is selected using only the permutation-based encoding. The candidate results can be identified, for example, by performing a k'-NN search in the permutation space (e.g. using the MI-File [14]) or by finding objects with a common permutation prefix (e.g. using the PP-codes [2]). We then refine the candidate result set by selecting the top-k candidate objects ranked according to a dissimilarity function (Figure 1). In order to use a dissimilarity function that does not require access to the original data, we propose to re-rank the objects based on their distances to a set of pivots. In fact, the distances between the objects and the pivots are calculated when computing the permutation-based representation and can therefore be easily reused at query time.

As done by many PBI approach [2, 14, 16], we consider the case in which the data objects are represented and indexed using permutation prefixes instead of the full-length permutations. We indicated with $PivotSet(\Pi_{o,l})$ the set of the l pivots closest to the object o, i.e. the pivots whose identifiers appear in the permutation prefix $\Pi_{o,l}$. Moreover, we assume that the distances between each object and its l closest pivots are stored and indexed within the object permutation prefix. This can be done with a slight modification of the used permutation-based index. In Figure 2, we show an example of how the object-pivot distances could be stored into posting lists such as the ones used in the MI-file [14]. Hereafter, we assume that the objects are indexed using this modified version of inverted files, however, the approaches presented in this paper can be extended to cope with different permutation-based indexes.

We propose to refine the candidate result set according to a dissimilarity function derived from the distance bounds provided either by the *Pivoted embedding* (Sec. 3.2) and the *nSimplex projection* (Sec. 3.3), since these metric mappings can be easily computed by using the object-pivot distances. Specifically, at query time, we use the distances $d(q, p_j)$, $d(o, p_j)$ with $p_j \in \Gamma_{o,q} = PivotSet(\Pi_{q,l}) \cap PivotSet(\Pi_{o,l})$ to calculate an approximation of the actual distance $d(o, q)$. In the following we present various distance approximation that can be used for this scope.

Pivoted embedding - The distance constraints expressed in the Equation 6 can be easily restricted to the pivots that belong to $\Gamma_{o,q}$:

$$\max_{p_j \in \Gamma_{o,q}} |d(o, p_j) - d(q, p_j)| \leq d(o, q) \leq \min_{p_j \in \Gamma_{o,q}} |d(o, p_i) + d(q, p_i)| \tag{8}$$

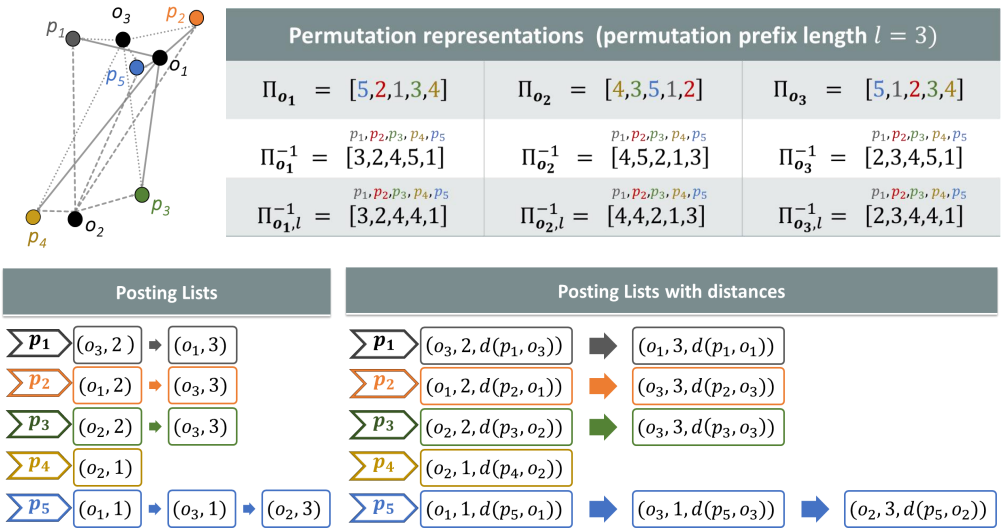

Figure 2: Examples of traditional posting lists and posting lists with distances, used to index three objects using five pivots and a prefix length $l = 3$

As a consequence, we identified three distance approximations that could be used to re-rank candidate objects:

$$P_{lwb}(o,q) = \max_{p_j \in \Gamma_{o,q}} |d(o,p_j) - d(q,p_j)| \qquad \text{lower-bound}$$

$$P_{upb}(o,q) = \min_{p_j \in \Gamma_{o,q}} (d(o,p_j) + d(q,p_j)) \qquad \text{upper-bound}$$

$$P_{mean}(o,q) = (P_{upb}(o,q) + P_{lwb}(o,q))/2 \qquad \text{mean}$$

Simplex projection - For each candidate object o, we use the pivots in $\Gamma_{o,q}$ to build the simplex base of the nSimplex projection $\phi_{\Gamma_{o,q}}$. Then we use the distances $d(o,p_j)$, $d(q,p_j)$ with $p_j \in \Gamma_{o,q}$ to project both the query and the candidate object into $\mathbb{R}^h$ where $h = |\Gamma_{o,q}| \leq l$. Given the projected apexes $\phi_{\Gamma_{o,q}}(o)$, $\phi_{\Gamma_{o,q}}(q)$, $\phi^-_{\Gamma_{o,q}}(q) \in \mathbb{R}^h$, we consider the re-rankings of the candidate objects based on the following dissimilarity measures:

$$S_{lwb}(o,q) = \ell_2(\phi_h(o), \phi_h(q)) \qquad \text{lower-bound}$$

$$S_{upb}(o,q) = \ell_2(\phi_h(o), \phi^-_h(q)) \qquad \text{upper-bound}$$

$$S_{mean}(o,q) = (S_{upb}(o,q) + S_{lwb}(o,q))/2 \qquad \text{mean}$$

Other dissimilarity functions over the apex vectors may be considered as well, in particular, any function that is always between the lower-bound and the upper-bound could be a good option since both the Simplex bounds asymptotically approach the true distance when increasing the number of pivots. In this work, we also consider the Zenith function, which was recently proposed in [29], that equals the quadratic mean of the lower- and upper-

bounds

$$S_{zenith}(o,q) = \sqrt{\left(S_{upb}(o,q)^2 + S_{lwb}(o,q)^2\right)/2} \qquad \text{zenith}$$

The main difference between the mean and zenith distance is that the latter has a geometrical interpretation as the Euclidean distance between two vertex in $\mathbb{R}^{h+1}$ (see [29] for futher details).

Note that number h of pivots used to build the simplex base highly affects the quality of the Simplex bounds: the higher h, the tighter the bounds. Moreover, the number h and the used simplex base change when changing the candidate object o. This means that the quality of the simplex-based approximations of the distance $d(o,q)$ may vary significantly when changing the considered candidate object. To overcome this issue, we also considered the re-ranking according to

$$S_{norm.mean}(o,q) = S_{mean}(o,q)/g(h) \qquad \text{normalized mean}$$
$$S_{norm.zenith}(o,q) = S_{zenith}(o,q)/g(h) \qquad \text{normalized zenith}$$

where $g(h)$ is a normalization factor, further discussed in Section 5.3.

Of all the measures considered above, only the lower-bounds S_{lwb} and P_{lwb} are metrics, while the others are dissimilarity functions. Finally, we remark that for all these approaches no new distance between object and pivot is evaluated neither at indexing time nor query time, since the distance used have already been calculated to build the permutation-based representations of the objects/query. The distances $d(o,p_j)$ with $p_j \in \Gamma_{o,q}$, instead, are retrieved while scanning the posting list to select the candidate results. Therefore, the considered re-ranking approaches do not require further disk accesses in addition to the index accesses already made to find the candidate results.

5. Experiments

In this section, we experimentally evaluate the quality of the re-ranking approaches discussed above. We first describe the employed data sets (Section 5.1) and other experimental settings (Section 5.2). Then, we report results and their analysis for several case studies (Sections 5.3-5.6)

5.1. Test Data

The experiments were conducted on three publicly available data sets, namely YFCC100M [30], Twitter-Glove [31], and SISAP Colors [32]. To test our techniques on a variety of metric spaces, for each data set we selected a different type of data descriptor and a different metric function, as described below.

YFCC100M is a collection containing about 96M images, all uploaded to Flickr between 2004 and 2014 and published under a CC commercial or non-commercial license. As image descriptors we used the deep Convolutional Neural Network features extracted by Amato et al. [33], which are publicly available at `http://www.deepfeatures.org/`. Those image descriptors are 4,096-dimensional vectors that were obtained from the activations

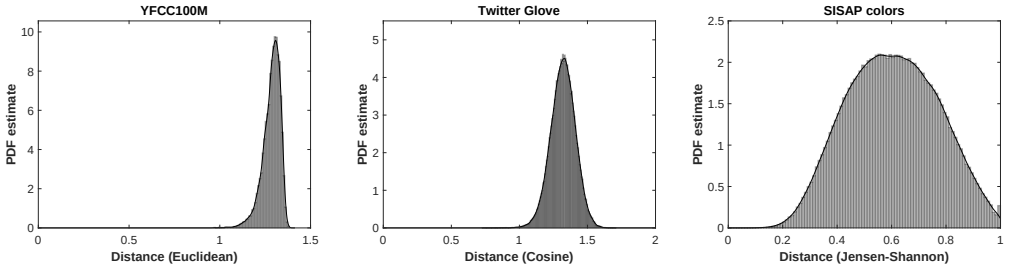

(a) *YFCC100M (*`IDim`*=* 276*)* (b) *Twitter-GloVe (*`IDim`*=* 106*)* (c) *SISAP Colors (*`IDim`*=* 8*)*

Figure 3: Probability density function estimated on a sample of 500,000 distances.

of the *fc6* layer of the HybridNet [34] after the ReLu and the ℓ_2 normalization stages. As commonly done in the literature, we used the *Euclidean distance* for the comparison of these features.

Twitter-GloVe is a collection of 1.2M GloVe [31] features (word embeddings) trained on tweets. The GloVe vectors are often used as vocabulary terms to embed a document into a vector representation, for example by averaging the vectors of the terms contained in the text. In such cases, the space of the vocabulary terms is representative of the space of the document embeddings. The Euclidean distance or the Cosine similarity are typically used to compare two GloVe vectors since they provide an effective method for measuring the linguistic or semantic similarity of the corresponding words. Various pretrained GloVe vectors are available at `https://nlp.stanford.edu/projects/glove/`. In our experiments, we used the 100-dimensional word vectors and we compared them using the *Cosine distance*, which is defined as $d_{\text{Cos}}(x, y) = \sqrt{1 - \frac{x \cdot y}{\|x\|_2 \|y\|_2}}$. Note that the Cosine distance is equivalent to the Cosine similarity, i.e. the closest objects to a query according to d_{Cos} are the most similar objects to the query according to the Cosine similarity.

SISAP Colors is a benchmark for metric search that contains about 113K feature vectors of dimensions 112. Each vector is a color histogram of a medical image. In our experiment, we compared those feature vectors by using the *Jensen-Shannon distance*, which is defined as the square root of the Jensen-Shannon divergence (JSDiv), i.e. $d_{\text{JS}}(x, y) = \sqrt{JS\,Div(x, y)}$. The term Jensen-Shannon divergence is used variously with slightly different meanings in literature; to avoid ambiguity, we follow the definition used in [8]:

$$JS\,Div(x, y) = 1 - \frac{1}{2} \sum_i h(x_i) + h(y_i) - h(x_i + y_i),$$

where $h(z) = -z \log_2 z$.

The distance distributions of the three considered data sets are depicted in Figure 3. In the figure captions we also report the Intrinsic Dimentionality (`IDim`) of the data that was estimated as in [35], i.e. `IDim`$= \frac{\mu^2}{\sigma^2}$, where μ is the mean and σ is the standard deviation of the distances between the data objects.

5.2. Experimental Setup

For each data set we build a ground-truth for the exact k-NN search related to 1,000 randomly-selected queries.[4] The ground-truths were used to evaluate the quality of the approximate results obtained by re-ranking a permutation-based result set of size $k' \geq k$. Specifically, for each query object we selected a candidate result set by performing a k'-NN search in the permutation space. Then we re-ranked the candidate results and we selected the top-k objects as the approximate answer to the k-NN query.

The quality of the approximate results was evaluated using the *recall@k*, defined as $|\mathcal{R} \cap \mathcal{R}^A|/k$, where $\mathcal{R}$ is the result set of the exact k-NN search in the original metric space and $\mathcal{R}^A$ is the approximate result set. We used $k = 10$ and $k' = 100$, thus the candidate result set was computed by performing a 100-NN search in the permutation space.

The permutation-based representations of the data objects were generated using a total of $n = 4,000$ pivots for YFCC100M and Twitter-GloVe data, and $n = 1,000$ pivots for the smaller SISAP Colors data set. In our tests, we used fixed-length permutation prefixes to represent the data objects. The permutation prefixes were compared using the *Spearman's rho with location parameter* metric, where the location parameter is the length l of the permutation prefixes. Note that the case $l = n$ simply corresponds to use of the full-length permutations with the traditional Spearman's rho metric. In the experiments, we evaluate the performance for various permutation prefix lengths.

5.3. Results

This section presents comparative results for all the approaches described in Sec. 4 to re-rank a permutation-based candidate results set. We remind the reader that the considered techniques are based on various `Pivoted embedding` and `Simplex projection` dissimilarity measures (namely, lower-bound, upper-bound, and mean), as well as the `Simplex` zenith function. We compared these approaches also with two baselines: 1) the permutation-based results before any re-ranking, 2) the re-ranking based on the actual distance. The permutation-based results before any re-ranking are simply the first k candidate objects ordered according to their permutation-based distance to the query (i.e. the k-NN results in the permutation space). A good re-ranking technique in terms of effectiveness should at least improve the recall of the permutation-based results, and ideally achieve a performance close to that obtained using the re-ranking based on the actual distance. In fact, the latter one is the approach that provides the maximum possible recall for the given candidate result set, but it requires to access the original metric object o to compute the distance $d(q, o)$ between the query q and every candidate object o.

Figure 4 illustrates the results on Twitter-GloVe and SISAP Colors data sets. Figures 5a and 5b show the results on two subsets of YFCC100M that contain 1M and 10M images, respectively. We used the term "`Perms`" to indicate the permutation-based results before any re-ranking, and "`Perms, re-rank(f)`" for the re-ranking based on the measure f, where f may be either the

- actual distance d,
- `Pivoted embedding` measures (P_{lwb}, P_{upb}, P_{mean}),

[4] The query objects were removed from the ground-truths of Twitter GloVe and SISAP Color data sets. For the YFCC100M we kept the query objects in the ground-truth to have results comparable with other research papers that used the same ground-truth (e.g. [19, 11]). Please also note that many re-ranking measures tested in this paper are not metrics, thus there are no guarantees that the less similar object to a query will be the query itself.

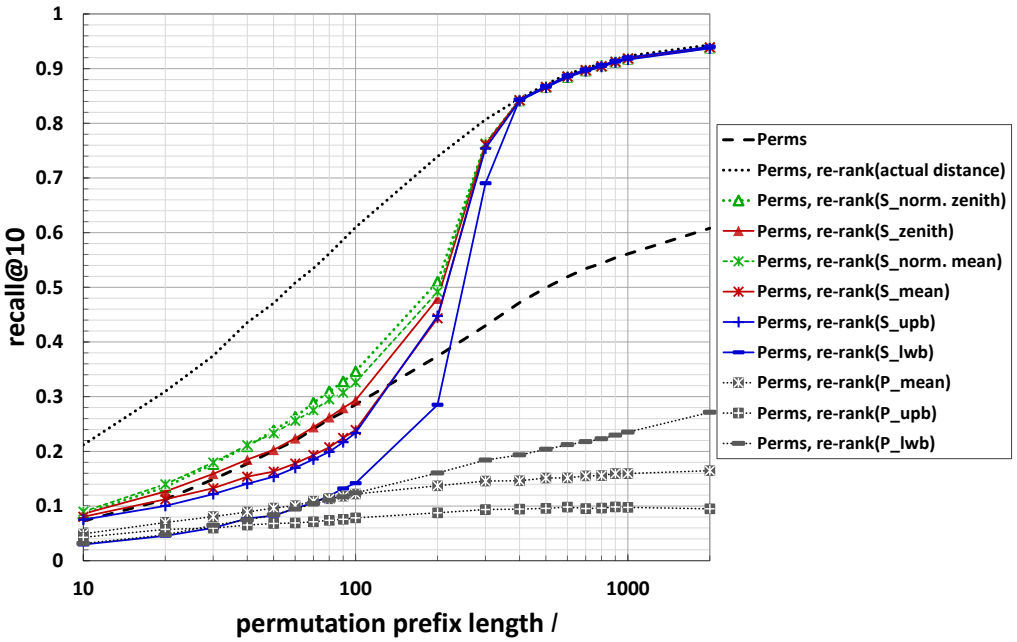

(a) `Twitter-GloVe, Cosine distance,` $n = 4,000$

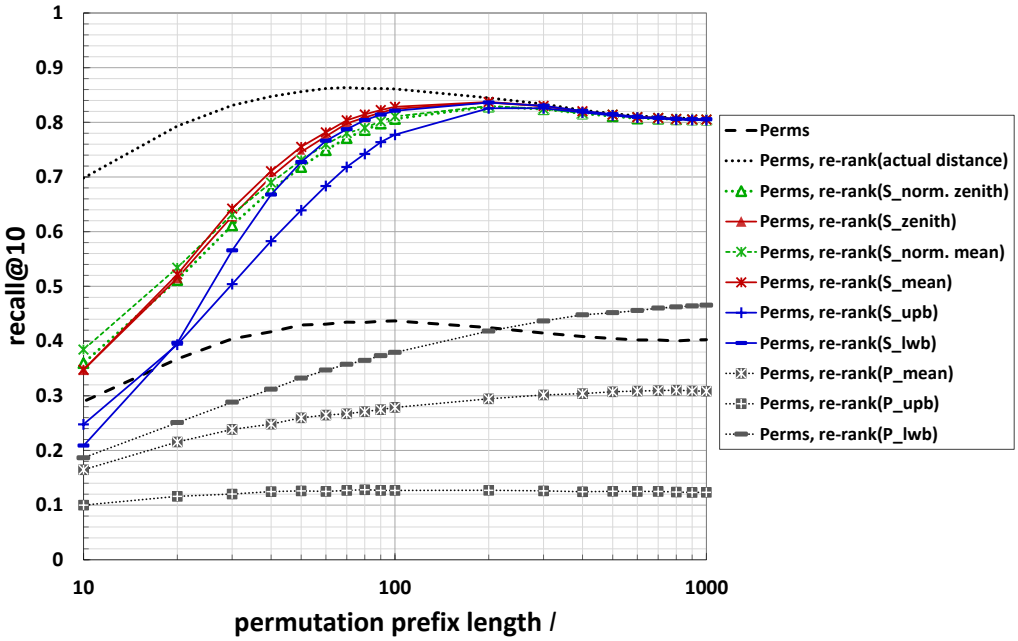

(b) `SISAP Colors, Jensen-Shannon distance,` $n = 1,000$

Figure 4: *Recall*@10 of several re-ranking approaches varying the permutation prefix length l. The candidate set to be reordered is selected with a 100-NN search in the permutation space using the Spearman's rho with location parameter l.

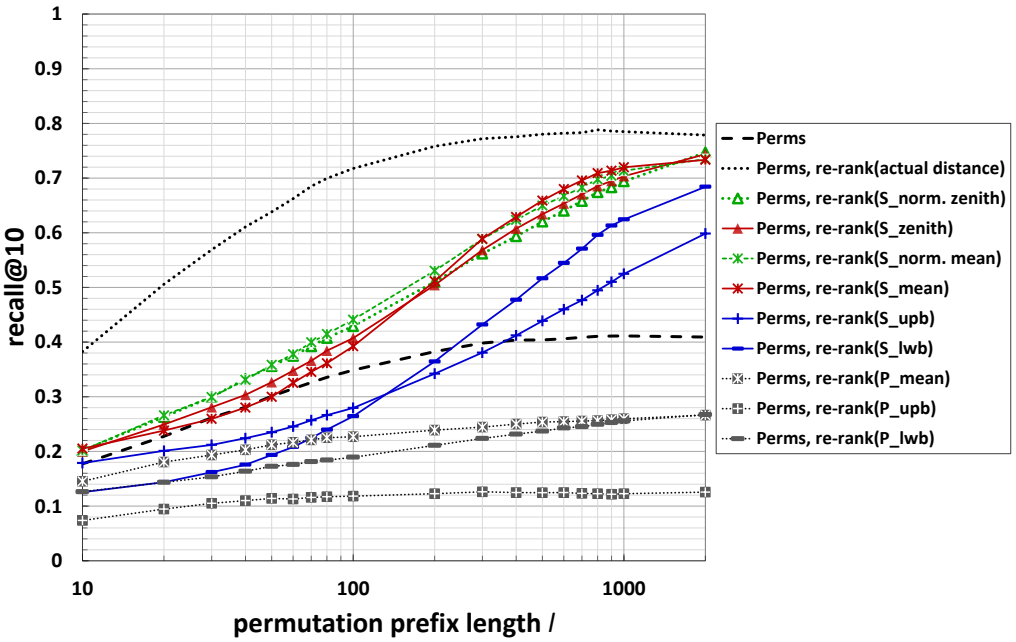

(a) Results on 1 million images

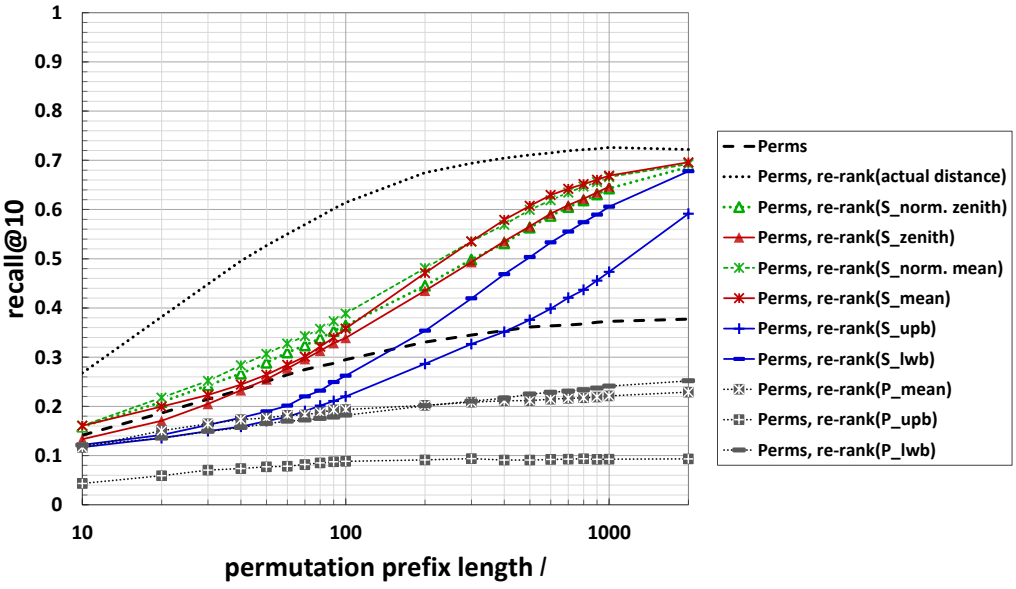

(b) Results on 10 million images.

Figure 5: `YFCC100M, Euclidean distance`: *Recall*@10 varying the permutation prefix length l on subsets of 1M images (5a) and 10M images (5b). The number of pivots is fixed to $n = 4,000$. The candidate set to be reordered is selected with a 100-NN search in the permutation space using the Spearman's rho with location parameter l.

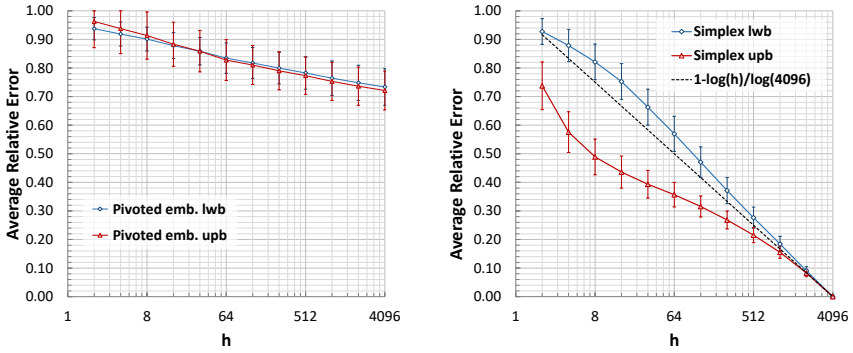

(a) `Pivoted embedding` (b) `Simplex projection`

Figure 6: YFCC100M, Euclidean Distance - Average relative error of the `Pivoted embedding` and `Simplex embedding` bounds with respect to the actual distance varying the number of h of pivots used to compute the bounds. Similar trends are obtained on Twitter-GloVe and SISAP colors data sets.

- `Simplex` measures (S_{lwb}, S_{upb}, S_{mean}, S_{zenith}, $S_{norm.mean}$, $S_{norm.zenith}$).

In each graph, we report the *recall*@10 varying the length l of the permutation prefixes used to represent the data objects (the number n of pivots is fixed). Please note that the prefix length l influences the quality of the candidate set to be re-ranked, as well as the quality of the `Pivoted embedding` and `Simplex projection` distance approximations. In fact, for a fixed value l and for a candidate object o, the number h of pivots used to compute the distance approximations is less than l; moreover, it varies and depends on the candidate object o as it is equal to the cardinality of $\Gamma_{o,q}$ (i.e. the intersection between the query permutation prefix and the object permutation prefix). Typically h is greater for objects in top positions in the permutation-based result list and decrease for objects that are far according to the permutation-based distance. Moreover, the greater the l, the greater the h and so the better the approximation bounds.

Surprisingly, we observed that in almost all the tested cases the `Pivoted embedding` approach greatly degrades the quality of the permutation-based results. Moreover, on YFCC100M and Twitter-GloVe it never reaches a *recall*@10 greater than 0.3. Hence, the `Pivoted` distance approximations resulted to be not adequate for the considered re-ranking purpose. One of the reasons for this poor performance is that the `Pivoted` lower-bound approximates well the actual distance $d(o,q)$ only if o and q are very close to each other in the original metric space, or if $\Gamma_{o,q}$ contains at least one pivot that is very close to q and far to o (or vice versa). However, for randomly selected pivots in high dimensional space this is unlikely to happen: for a random pivot p and for an object o not so close to q, we often have that the distances $d(o,p)$ and $d(q,p)$ are both close to the mean value in the distribution of the data distances, and so the lower-bound results to be close to zero. This means that when we use the `Pivoted` lower-bound for re-ranking purpose, it may happen that many objects are incorrectly swapped and far objects can be assigned in top-positions. In addiction, we observed that the `Pivoted` distance bounds have high relative errors with respect to the actual distance and that these errors slightly decrease when increasing the number h of pivots used to compute the bounds (Figure 6a).

The `Simplex` distance bounds showed similar drawbacks when using relatively small prefix

lengths. In particular, they are mostly influenced by the fact that the `Simplex` bounds asymptotically approach the true distances when increasing the number h of pivots used to build the simplex base and that the tightness of the bounds highly depends on h. In fact, in all the tested cases, we observed that there exists a value $\tilde{h}$ for which the full convergence is achieved. This value is 4,096 for YFCC100M, and about 100 for Twitter-GloVe/SISAP Colors. The effect of the convergence of the `Simplex` bounds is evident in both the Twitter-GloVe (Figure 4a) and the SISAP Colors (Figure 4b) data: for $l > 300$ we observed that the number of pivots in the intersection $\Gamma_{o,q}$ starts to exceed $\tilde{h} = 100$ for most of the candidate objects o, and so all the `Simplex` bounds provide an exact or almost exact approximation of the actual distances. As a consequence, for $l > 300$ all the recall curves of the `Simplex`-based re-ranking approaches coincide with the recall curve obtained using the re-ranking based on the actual distance. For the YFC100M data set, instead, the `Simplex` bounds recall curves do not reach the values obtained by using the actual distance because we are considering prefix lengths smaller than the number $\tilde{h}$ of pivots needed to have the convergence.

We remark that the performance of the `Simplex` bounds is poor for *small prefix lengths* mainly because

- for two objects $o, s \in CandSet(q)$ such that $|\Gamma_{o,q}| < |\Gamma_{s,q}| << \tilde{h}$ we may have $S_{lwb}(o,q) < S_{lwb}(s,q)$ even if $d(o,q) > d(s,q)$;
- the upper-bound, which is not a metric, particularly fails in approximate small distances and $S_{upb}(o,o)$ may be much greater than 0.

This behaviour of the S_{upb} is somehow observable in the recall values obtained on the YFFCC100 data: for small l the results of the re-ranking based on the S_{upb} are better than that of S_{lwb} on the 1M images subset (Fig. 5a), but on 10M images (Fig. 5b) the curve of S_{upb} never exceeds that of S_{lwb}. The reason is that the actual distances between the query and the candidate objects are likely to be smaller when performing the nearest neighbour search on a lager subset of data. Thus, given that for small prefix lengths the S_{upb} does not approximate well tiny distances, the performance of the re-ranking based on the upper-bound drops when the candidate objects are selected by searching 10M images.

It is worth noting that, accordingly to our experimental observations, if we use the same simplex base (e.g. the one formed by the pivots in the query permutation prefix) to project all the candidate objects, we achieve re-ranking scores better than that showed in the Figures above, especially for relatively small prefix lengths. However, this approach is not directly applicable in the analysed scenario. In fact, we used inverted files to index the permutations and store the distances object-pivots. This implies that at query time, for each candidate object o we had access only to the distances $d(o,p)$ with p appearing in both the object and query permutation prefixes. Therefore, the set of pivots employed to build the simplex base changes when considering different candidate objects. This means that the "quality" (tightness) of the `Simplex`-based approximations of the query-object distances is not uniform within the set of the candidate objects. To overcome this issue, we tested normalized versions of all the `Simplex` distance bounds by taking into account the number h of pivots used for projecting the data. In the graphs reported in this paper, we show only the normalized version of the mean and zenith distances since they were the ones obtaining the best results. As normalization factor we used $g(h) = \log(h)$ because we experimentally observed that the relative errors of the Simplex bounds decrease logarithmically with h (e.g. Figure 6b).

The re-rankings based on the normalized versions of the `Simplex` mean and zenith have practically the same performance on Twitter Glove and SISAP Colors data sets, while on YFCC100M data the $S_{norm.mean}$ shows slightly better recall values. Moreover, in all the tested cases, the re-rankings using those `Simplex` measures always improved the permutation-based results (i.e. the `Perms` baseline). For example, for $n = 4,000$ pivots and $l = 800$, the *recall*@10 is improved from 0.37 to 0.64 on YFCC100M (10M subset). For $n = 4,000$ and $l = 300$, the recall increases form 0.43 to 0.76 on Twitter-GloVe, while for $l = 80$ and $n = 1,000$ it raises from 0.43 to 0.80 on SISAP Colors. We provided examples with $l < n$ instead of considering the full-length permutation since when using inverted files the number of index blocks accessed is proportional to l^2/n and does not depend on the number of retrieved objects. Moreover, it is worth to note that the quality of permutation-based results it is not always improved by considering large prefix lengths. In fact, it often happens that there exists an optimal prefix length for which we achieve a recall that is better or very similar to that obtained using the full-length permutations. This phenomenon is observable in the YFCC100M and the SISAP Colors data set (see Fig. 5 and 4b), where the `Perms` recall line has a plateau or decreases after achieving a maximum value. Other examples of this phenomenon can be found e.g. in [18] where it was observed the existence of an optimal prefix length $l < n$ for some synthetic and real-word data sets. The intuition is that in those cases the intrinsic complexity of the data set is already well described when permutation prefixes with length equal to the optimal value are used, therefore increasing the length of the prefixes may add noisy information instead of improving the data representation. This phenomenon is not yet completely investigated in the literature, however, we mentioned it to clarify why in the SISAP Colors case the performance is affected by using a large l parameter.

Finally, we observe that the cost of the considered re-ranking approaches depends on the query object as it changes according to the numbers of pivots in the intersections of permutation prefixes of the query and the candidate objects. If using the algorithm proposed in [10], the cost for building a simplex base using h pivots is $O(h^3)$ floating point operations (flops), while the cost for projecting an object is $O(h^2)$ flops. Thus, for k' candidate objects whose permutation prefixes have on average h_l pivots in common with the query permutation we have a cost of $O(k'(h_l^3 + h_l^2) + h_l^2)$ flops to compute the `Simplex` bounds. However, the k' simplex bases can be computed in parallel since they referred to different sets of pivots. Just to provide an example, for $l = 300$ the time cost for computing all the simplex bases and projecting both the query and the candidate objects is about 300ms on an Intel i7 3.5 GHz for the YFCC100M data. We also observe that this cost may be greatly reduced if some of these simplex bases are pre-computed or partially computed. In facts, if we have a simplex base built upon the pivot set $\{p_{i_1}, \ldots, p_{i_h}\}$ and we extend it by adding a further pivot the cost is $O(h^2)$ flops instead of the $O(h^3)$ flops needed to build it from scratch. Therefore, implementations that exploit hashmaps or prefix trees to dynamically cash the computed simplex bases would accelerate the response at query time.

5.4. Results on Large Scale

To evaluate our techniques on large scale, we performed the k-NN search on various subsets of YFCC100M. Figure 7a shows the *recall*@10 varying the data set size from 1 to 96 million images. The candidate results to be re-ranked were selected by using permutation prefixes of length $l = 800$. We observe that the performance of our techniques with respect to the `Perms` and `re-rank(actual distance)` baselines is stable when increasing the size of the data set. In particular, the *relative improvement* in the recall obtained by the `Simplex` mean and zenith re-rankings with respect to `Perms` results ranges between 70% (at 96M) and 78% (at 8M). Moreover,

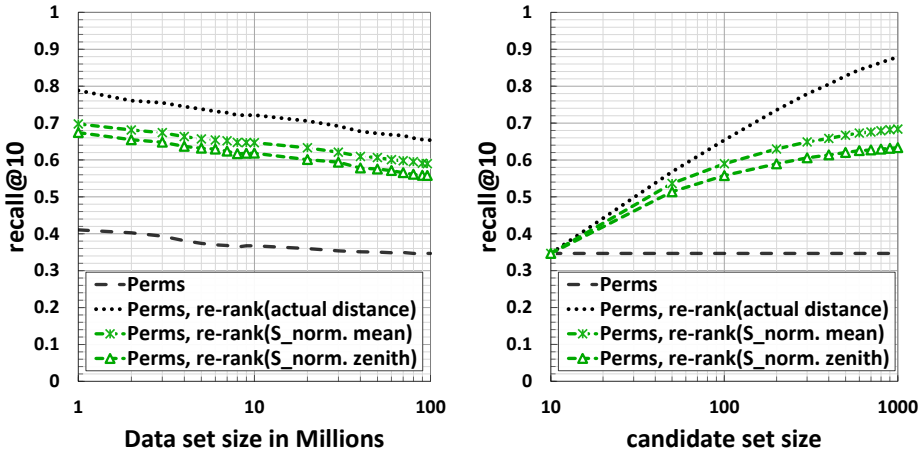

(a) Recall@10 varying the data set size

(b) Recall@10 varying the candidate set size (full YFCC100M dataset)

Figure 7: `YFCC100M, Euclidean distance,` $n = 4000$, $l = 800$

for large sizes of the data set the relative gap between our techniques and the re-ranking based on the actual distance slightly decreases.

We also investigated the performance varying the size k' of the candidate set to be re-ranked (Figure 7b). In this case, the candidate set was selected by performing a k'-NN search in the permutation space using the Spearman's rho with location parameter $l = 800$. As expected, the gap between our approaches and the re-ranking based on the actual distance increases for large sizes of the candidate set due to the errors in approximating the actual distance by the `Simplex` measures. In facts, for the considered parameter $l = 800$, on average we have about 550 pivots in the intersection between the query and the object permutation prefixes, but for the YFCC100M data set the convergence of the Simplex bounds is achieved using 4,096 pivots. Thus, the effects of distance approximation errors becomes more evident when we re-rank larger set of data. Nevertheless, even when considering $k' = 1,000$ as candidate set size, the improvements in the recall of our approach with respect to the `Perms` baseline is considerable (from 0.35 to 0.59)

Finally, Figures 8 and 9 show some examples of 10-NN search results on a 10 million subset of YFCC100M deep features. Specifically, these results were obtained by using

1. the permutations compared with the Spearman's rho with location parameter l ($S_{\rho,l}$) without any re-ranking step (see Fig. 8b and 9b),
2. our approach for re-ranking the permutation-based results using the nSimplexnormalized mean ($S_{norm.mean}$) measure (see Fig. 8c and 9c),
3. brute-force, i.e. the exact search via sequential scan using the Euclidean distance (ℓ_2) for the image features comparison (see Fig. 8d and 9d).

We considered the case $l = 800$ and we selected two query examples (Fig. 8a and 9a) for which our technique achieved the worse and the best *recall*@10 over all the $1,000$ tested queries, which are 0.1 (Fig. 8c) and 1 (Fig. 9c) respectively. In the first example, it is interesting to note that even if the recall of our technique is very low, from a visual similarity point of view our

(a) **Query** (id: 3528451473)

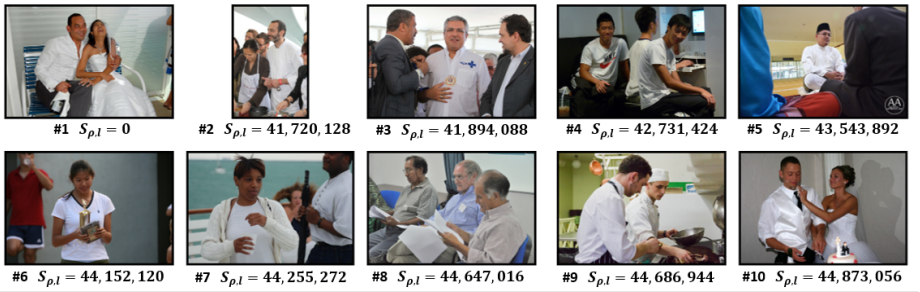

(b) **Perms**, *recall*@10 = 0.1

(c) **Perms, re-rank(Simplex Normalized mean)**, *recall*@10 = 0.1

(d) **Exact search via sequential scan** (Ground-truth)

Figure 8: Example of 10-NN search results obtained on 10 million images of YFCC100M using the permutations without any re-ranking (b), our Simplex re-ranking technique (c), and the sequential scan (ground-truth) (d).

(a) **Query** (id: 9330452712)

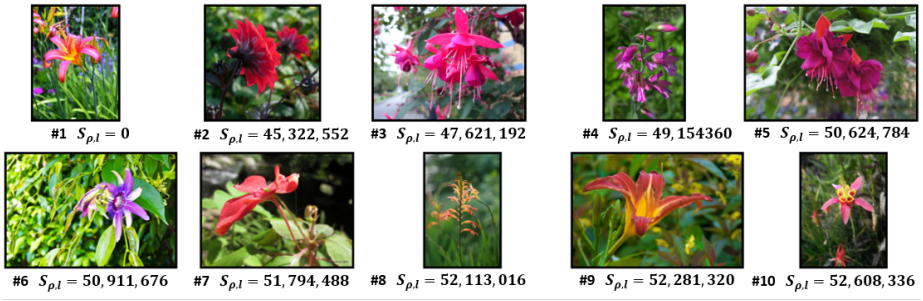

(b) **Perms**, $recall@10 = 0.3$

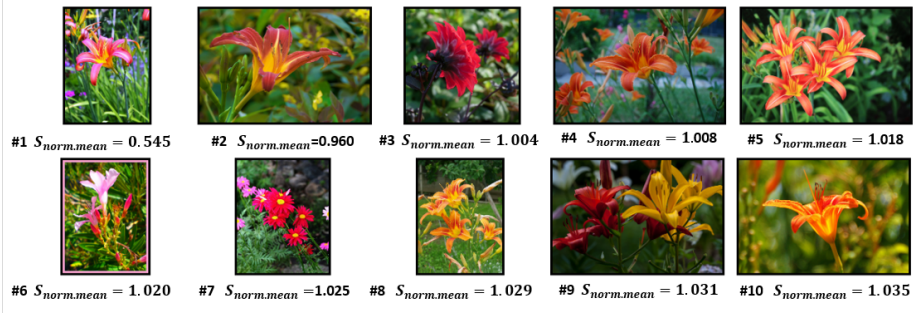

(c) **Perms, re-rank(Simplex Normalized mean)**, $recall@10 = 1$

(d) **Exact search via sequential scan** (Ground-truth)

Figure 9: Example of 10-NN search results obtained on 10 million images of YFCC100M using the permutations without any re-ranking (b), our Simplex re-ranking technique (c), and the sequential scan (ground-truth) (d).

Table 2: Intrinsic dimensionalities for experimental Euclidean spaces

Dim	IDIM
10	10.23
20	20.85
30	31.24
40	42.18
50	52.98
60	63.31
70	75.05

Dim	IDim
80	85.93
90	95.35
100	106.35
200	212.55
300	319.80
400	423.71
500	525.78

results are not so worse than the ground-truth images. The second example shows a case in which we achieved the maximum recall (1.0), allowing us to highly improve the recall obtained by the permutation-based search (0.3). Note that in this case, even though the set of our results coincides with the ground-truth set, the ordering of the results is different because for $l = 800$ the `Simplex` bounds are not converged yet to the actual distance.

A demo of the k-NN search results on YFCC100M for various data set sizes (from 1 to 96M) and various re-ranking approaches is available at the link `http://deepfeatures.org/rerankingPerms/`.

5.5. Results for Increasing Data Dimensionality

To evaluate the performance of our technique as the intrinsic dimensionality of the data rises, we conducted experiments on 14 synthetic data sets. Specifically, we generated pseudo-random data sets of half million vectors with Gaussian distributed values within $\mathbb{R}^D$ with $D \in \{10, 20, 30, 40, 50, 60, 70, 80, 90, 100, 200, 300, 400, 500\}$. Table 2 gives values for the intrinsic dimensionality (IDim) calculated for each space. The IDim was computed as proposed in [35], that is IDim= $\mu^2/2\sigma^2$ where μ and σ are, respectively, the mean and the standard deviation of the distances between points of the space.

For each space, we evaluated the *recall*@10 obtained by re-ranking the permutation-based results. As proposed in [14], we computed the permutation-based representations by using a number of pivots greater than twice the size of the data set. Specifically, we used $2,000$ pivots for each set of data. Then, we varied the prefix length from 10 to 1000 using a logarithmic scale, i.e. we considered l =10, 20, 30, 40, 50, 60, 70, 80, 90, 100, 200, 300, 400, 500, 600, 700, 800, 900, 1000. For each data set and each prefix length l we evaluated the recall achieved by various re-ranking approaches. In Figure 10, we reported the results for the permutation-based search without any re-ranking, and the results for the re-ranking based either on the nSimplex normalized mean measure or the actual distance. For all the tested spaces and prefix lengths, our technique improved the recall obtained using the `Perms` baseline. Moreover, we experimentally observed that when the prefix length l was three times the dimensionality of the data, our re-ranking techniques achieved the same recall as the re-ranking based on the actual distance. On average the relative improvement of our re-ranking approach over the `Perms` baseline decreases as the spaces become less tractable, that is as the intrinsic dimensionality increases. However, for large prefix lengths our technique still achieves the same performance of the re-ranking based on the actual distance. Note that for data with very high intrinsic dimensionality the recall values are very low due to the less tractability of the space. For example, on the Euclidean space of

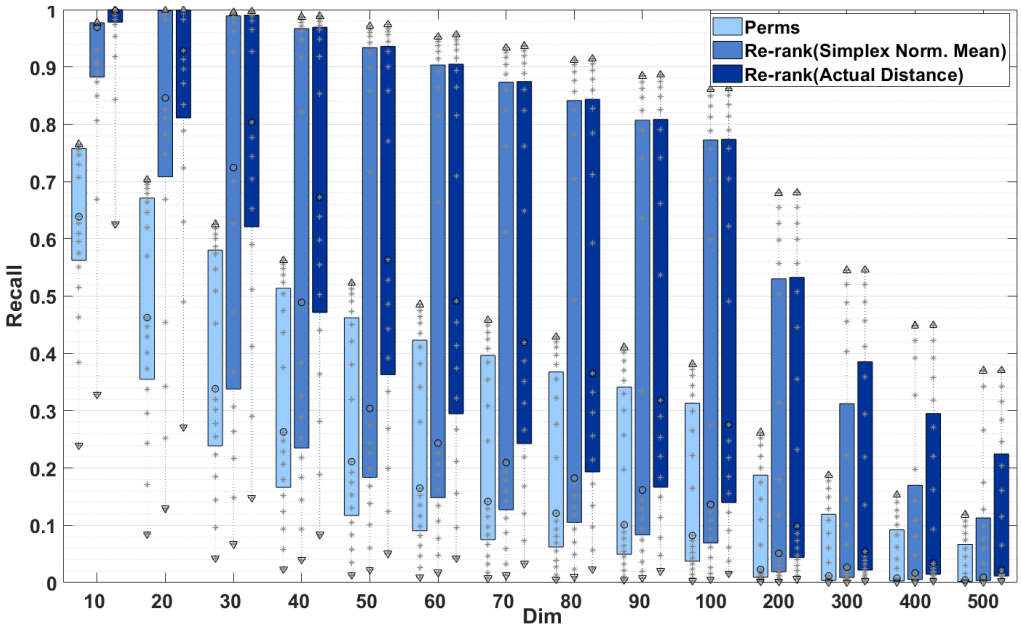

Figure 10: Recall@10 obtained by searching synthetic Euclidean spaces of various dimensionalities (from 10 to 500) varying the re-ranking approach and the permutation prefix length l. For each data set and each re-ranking technique, the graph shows 19 grey points ($*$) that are the recall values obtained varying l form 10 to 1000 (logarithmically increasing values) and a box-plot displaying the distribution of these values. Each box is delimited by the first and the third quartile, $\triangle$ is the maximum value (corresponding to $l = 1,000$), $\triangledown$ is the minimum value (corresponding to $l = 10$), $\circ$ is the median value (corresponding to $l = 100$).

dimension 500, the maximum recall (achieved with $l = 1,000$) is 0, 12 for the `Perms` without re-ranking and 0, 37 for the re-ranking based either on the nSimplex measure or the actual distance. We also noticed that for relatively small IDim (e.g. $dim = 10, 20$) and for small prefix lengths, the results obtained using the re-ranking based on the nSimplex mean and zenith measures achieved much better results than that obtained using their normalized version. However, in our tests, the nSimplex normalized measures worked the best for $dim > 30$.

5.6. Results using quantized distances

In the experiments analysed so far, the object-pivot distances used to perform the re-rankings were indexed within the object permutation prefixes by using inverted files (as discussed in Section 4). The disk space needed by the inverted index can be estimated in general assuming to encode each entry of the posting lists with $\lceil log_2|X| \rceil + 32$ bits, where $|X|$ is the size of the data set. This space is largely sufficient to encode both the ID of the object and its distance from the pivot corresponding to the list to which the entry belongs to. As observed in [14], the positions of the objects can be neglected by ordering the entries of the posting list according to the position of the objects. Therefore, for a fixed l, the size of the inverted index used by our approaches is $l|X|(\lceil log_2|X| \rceil + 32)$ bits. For reference we also observe that (i) the size of the inverted index of the `Perms` approach (i.e. the one that does not store the distances) is $l|X|(\lceil log_2|X| \rceil)$ bits; (ii)

Table 3: Examples of disk space in Gigabytes needed by various approaches to index and search the YFCC100M data set using inverted files. The re-ranking based on the Simplex measures requires to store the object-pivot distances within the permutation prefixes. The re-ranking based on the actual distance needs to store the permutation prefixes as well as the original data.

Approach	**Disk space (GB)**			
	1M deep features		100M deep features	
	$l = 300$	$l = 800$	$l = 300$	$l = 800$
`Perms`	0.7	1.9	94.3	251.5
`Perms,re-rank(actual dist.)`	16.0	17.1	1620.5	1777.7
`Perms,re-rank(Simplex)`	1.8	4.8	206.1	549.5
`Perms,re-rank(Simplex)` with distances quantized to 8 bits	1.0	2.6	122.2	326.0

the search approach relied on the re-ranking of the permutation-based results according to the actual distance requires to store both the `Perms` index and the original data set, thus it needs $l|X|(\lceil log_2|X|\rceil) + |X|(\lceil log_2|X|\rceil + D * 32)$ bits, if the data objects are D-dimensional real-valued vectors.

For example, the disk space required to index and search 1M deep fearures ($D = 4,096$) of YFCC100M using permutation prefixes of length $l = 300$ are about 1.8 GB for our techniques, 0.7 GB for the `Perms` approach, and 16 GB for the `Perms, re-rank(actual distance)` technique (see also Table 3).

Since the re-rankings based on the nSimplex measures or on the actual distance need to store more information than the `Perms` baseline, to have a fair comparison we show in Figure 11 the recall obtained on 10M images of YFCC100M as a function of the disk space used. We observed that the the only case in which the performance of the `Perms` baseline is better then our approach is when we use indexes with very limited size. However, in that case the achieved recall does not exceed 0.3. For all the other cases, our re-reranking approach showed the best compromise between used disk space and recall. Nevertheless, our approach would be even more advantageous if we were able to achieve the same effectiveness but reducing the disk space used to store distances.

To reduce the size of our inverted index, we investigated the idea of compressing the posting lists by storing quantized distances. Since the quantized distances are then used to compute the Simplex projection of the data objects, the performance of our re-ranking techniques may degrade due to the quantization errors. We investigated this aspect by testing several floating-point quantization approaches in conjunction with our Simplex-based re-ranking technique. Specifically, for a value x in a finite range (x_{min}, x_{max}) we tested the following scalar quantizers.[5]

Uniform quantizer is probably the simplest type of quantizer. It divides the interval (x_{min}, x_{max}) into L intervals of the same length $Q = (x_{max} - x_{min})/L$. Each value x is then mapped to the middle value of the interval it belong to, i.e.,

$$q_{unif}(x) = x_{min} + Q/2 + Q\lfloor (x - x_{min})/Q \rfloor \tag{9}$$

[5]Note that in our case $x_{min} = 0$ since we are considering distance values.

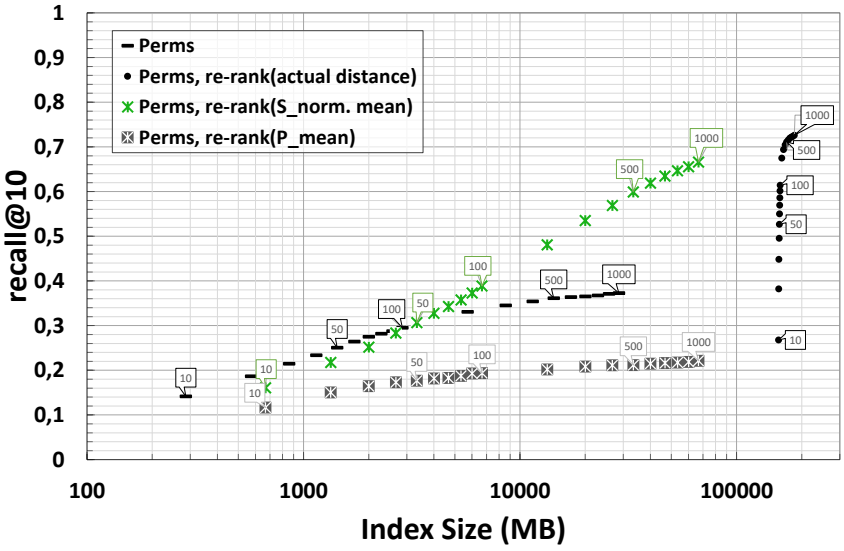

Figure 11: `YFCC100M (10 million images subset), Euclidean distance`: *Recall*@10 as a function of the disk space used to store the index/features by various re-ranking techniques. For each approach that graph shows the results varying the prefix length l from 10 to 1000.

Nonuniform quantizer is typically modeled as a cascade of a non-linear mapping (*compressor*) followed by a uniform quantizer and an inverse non-linear mapping (*expander*). The non-linear mapping before the uniform quantization allows us to keep the number of quantization intervals constant but differentiating the size of those intervals so as to better to approximate the input in certain regions (e.g. regions that have more probability mass). We considered the following nonuniform quantizers:

μ-law quantizer uses the μ-law mapping as compressor function, which is defined as

$$F_\mu(x) = V \frac{\log\left(1 + \mu \frac{|x|}{V}\right)}{\log\left(1+\mu\right)} \text{sign}(x) \tag{10}$$

where $V = \max\{|x_{min}|, |x_{max}|\}$, and μ is a compression parameter (e.g. $\mu = 255$ is used in the North American and Japanese standards for digital telecommunication signals). The transformed values are then quantized using a uniform quantizer for the trasformed interval. Thus, the final quantized value associated to x is $q_{unif}(F_\mu(x))$.

To transform a quantized value y back, we use the inverse μ-law:

$$F_\mu^{-1}(y) = \frac{V}{\mu}\left((1+\mu)^{|y|/V} - 1\right)\text{sign}(y). \tag{11}$$

Since the values close to zero are less compressed than values with greater absolute values (the quantization intervals increase logarithmically), usually the values are mean-centered before the quantization.

Table 4: Results of various quantization approaches (YFCC100M data set). The quantizers are applied to the distances of the data objects to their l nearest pivots, i.e. the distances store in the posting lists. The reported results were obtained using the `Perms,re-rank`($S_{norm.mean}$) approach, distance quantized to 8 bits, and permutation prefixes of length $l = 800$.

Quantizer	**Compressor parameter**	**MSE**	**recall@10**
Uniform		3.24E-03	0.228
μ-law	$\mu = 48$	2.64E-07	0.698
A-law	$A = 3$	1.04E-06	0.696
No quantization		0	0.698

A-law quantizer uses the A-law compressor, which is defined as

$$F_A(x) = V\text{sign}(x) \begin{cases} \dfrac{A|x|/V}{1+\ln(A)} & |x| < V/A \\ \dfrac{1+\ln(A|x|/V)}{1+\ln(A)} & V/A \leq |x| \leq V \end{cases} \tag{12}$$

where A is a compression parameter and $V = \max\{|x_{min}|, |x_{max}|\}$. The compressed values are then quantized using an uniform quatizer. The mapping used as expander is the inverse A-law:

$$F_A^{-1}(y) = \frac{V\text{sign}(y)}{A} \begin{cases} \dfrac{|y|}{V}(1+\ln(A)) & |y| < \dfrac{V}{1+\ln(A)} \\ \exp(\dfrac{|y|}{V}(1+\ln(A)) - 1) & \dfrac{V}{1+\ln(A)} \leq |y| < V \end{cases} \tag{13}$$

Also in this case the data are centered before the quantization.

The number L of intervals we used for each quantizer is $L = 2^{\text{nBits}}$, where `nBits` are the number of bits used to store each distance. For each approach, we computed the *Mean Squared Error* (MSE) on a sample set of data. The MSE is a frequently used to evaluate how close are the (reconstructed) quantized values x' to the original values x, and it is defined as $\frac{1}{m}\sum_{i=1}^{m}(x_i - x'_i)^2$, where m is the number of samples.

For the μ-law and A-law quantizer, we select the optimal μ and A parameters as the ones providing us the lowest MSE over a sample set of object-pivots distances. We then evaluate the recall obtained by re-ranking the permutation-based candidate set according to the Simplex bounds computed using the quantized distances. Table 4 shows comparative results on 1M subset of YFCC100M using a prefix length of $l = 800$ and `nBits` = 8.

As expected the uniform quantizer has really poor results since the distribution of the distances is not uniform. The tested nonuniform quantizers have results similar to each other. We decided to use the μ-law quantizer since it showed slightly better results.

We then thoroughly tested the performance of our technique by varying the data set, the permutation prefix length l, and the number of bits used to store each object-pivot distance. Figures 12, 13, and 14 illustrate the results on YFCCC100M, SISAP Colors, and Twitter GloVe, respectively. For the sake of simplicity, we show results obtained using a fixed parameter μ for all tested permutation prefix lengths. This parameter was selected as the one minimising the MSE

error in approximating the distances of the objects to all the n pivots. In facts, we observe that results obtained in this way are practically equivalent to that obtained by estimating an optimal parameter μ for each different choice of the parameter l.

On YFCC100M (Euclidean distance) and SISAP Colors (Jensen-Shannon distance), we were able to satisfactorily preserve the quality of the re-ranked results when using at least 8 bits to store each distance. However, we observed a huge degradation when using fewer bits. For example, the re-ranked results became worse than the permutation-results when we use less than 5 bits. The problem is that the quantized object-pivot distances are then used to compute the Simplex projection of the object, so the quantization errors propagate in the Simplex-based estimation of the query-object distance. The effect of this error propagation is more evident in Twitter Glove data (cosine distance), where the results obtained for $l \geq 300$ is highly degraded using quantized distances. On this data set, we needed about 14 bits to preserve the quality of the re-ranked results even though the MSE errors related to distances quantized using fewer bits were in line with that obtained in the other tested data sets.

6. Conclusions

In this article, we presented an approach that exploits a pivot-based local embedding to refine a set of candidate results of a similarity query. We focused our attention on refining of a set of approximate nearest neighbour results retrieved using a permutation-based search system. However, our approach can be generalized to other types of approximate search provided that they are based on the use of anchor objects (pivots) from which we pre-calculate the distances for other purposes. For example, some data structures use inverted indices, as the inverted multi-index [36], in which objects belonging to a Voronoi cell are inserted in a posting list associated with the centroid of the cell from which we calculated the distance. Other indexes that can benefit from our approach are those based on permutation prefix trees, like PP-Index [2] and PPP-Index [16].

The core idea of the proposed technique is using the distances between an object and a set of pivots (pre-computed at indexing time) to embed the data objects in a metric space where it is possible to compute upper- and lower-bounds for the actual distance. Dissimilarity functions defined upon those bounds are then adopted for re-ranking the candidate objects. The main advantage is that the proposed approach does not need to access the original data as done, instead, by the most commonly used refining technique that relies on computing the actual distances between the query and each candidate object.

We analysed the refining based on two data embeddings, namely the Pivoted embedding and the nSimplex projection, and several dissimilarity functions derived by these space transformations. The refining approaches using the nSimplex projection resulted to be particularly effective for refining permutation-based results. For example, using the refining according to the nSimplex normalized mean function, we were able to almost double the precision of the permutation-based results even on a data set of about 100 million objects.

Acknowledgements

The work was supported by Smart News, "Social sensing for breaking news" (CUP CIPE D58C15000270008), VISECH ARCO-CNR (CUP B56J17001330004), and AI4EU project (funded by the EC, H2020 - Contract n. 825619).

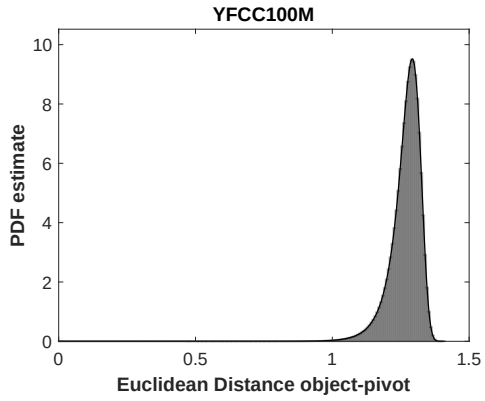

(a) Probability distribution of the distances between the data objects and the n pivots

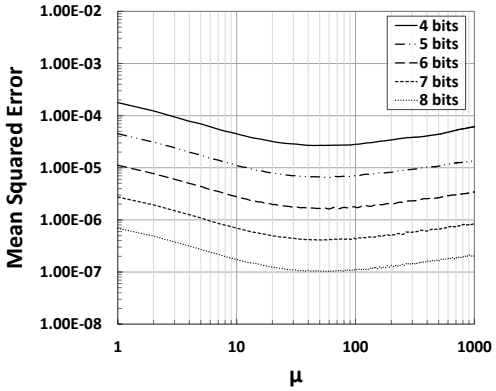

(b) Mean Squared Error for the μ-law quantization varying μ

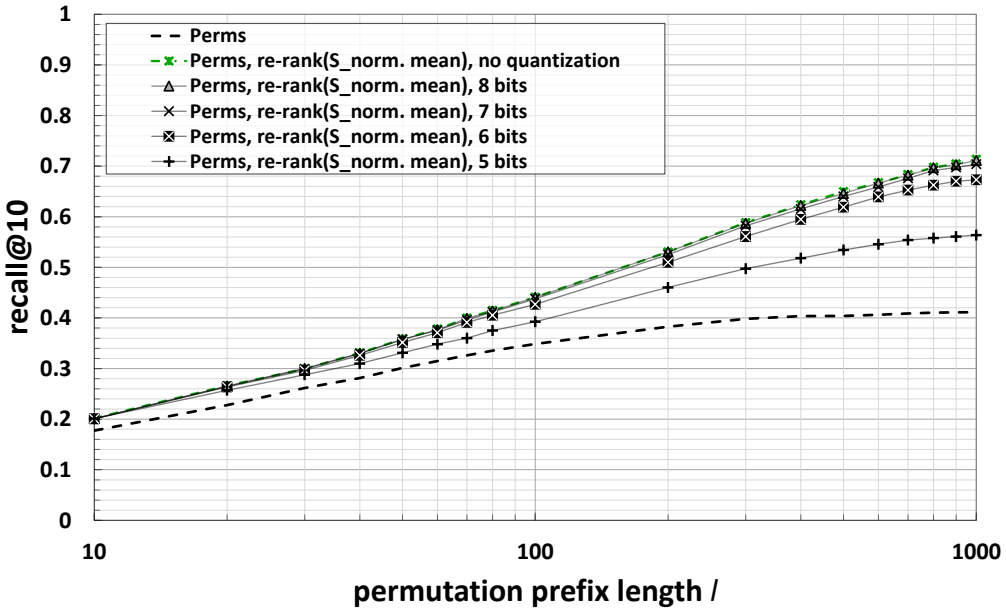

(c) *Recall*@10 varying the permutation prefix length l ($\mu = 57$)

Figure 12: *YFCC100M (1M), Euclidean distance,* $n = 4,000$ *pivots*

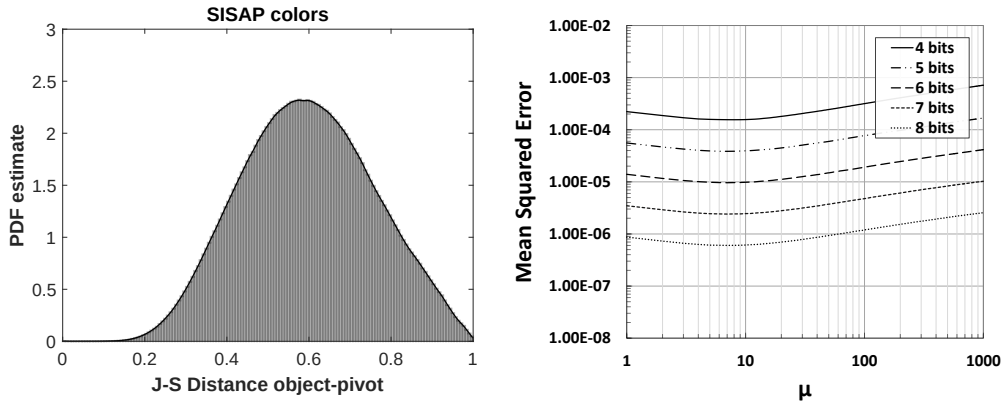

(a) Probability distribution of the distances between the data objects and the n pivots

(b) Mean Squared Error for the μ-law quantization varying μ

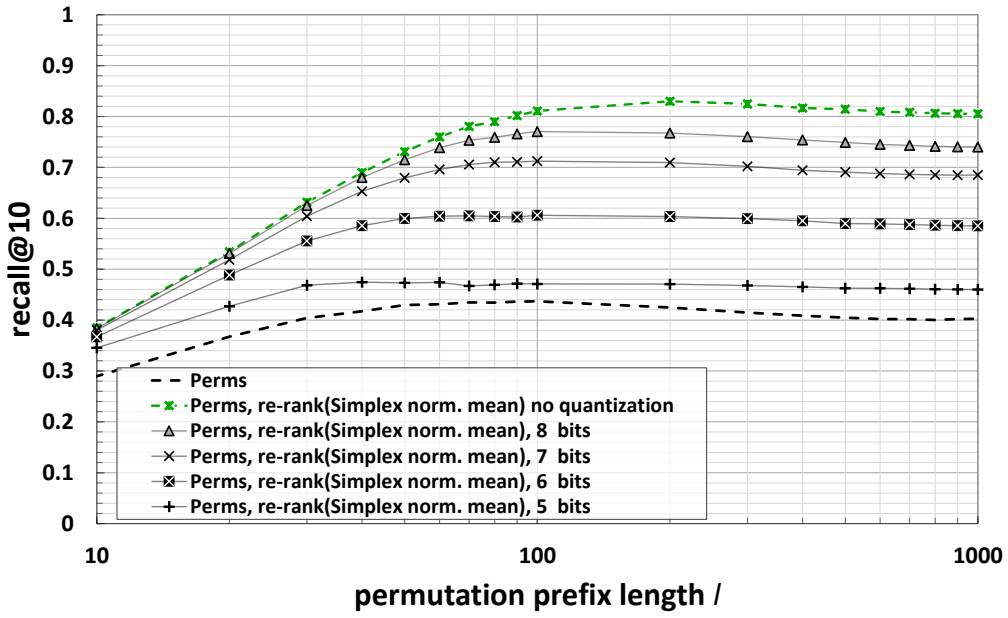

(c) *Recall*@10 varying the permutation prefix length l ($\mu = 3$)

Figure 13: *SISAP colors, Jensen-Shannon distance,* $n = 1,000$

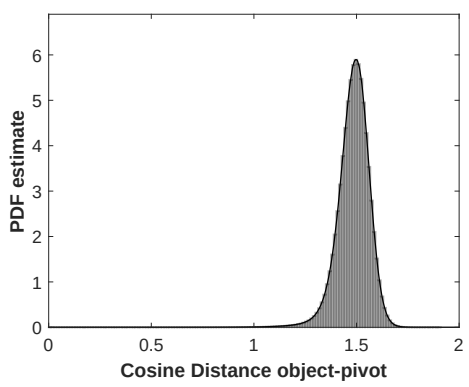

(a) Probability distribution of the distances between the data objects and the n pivots

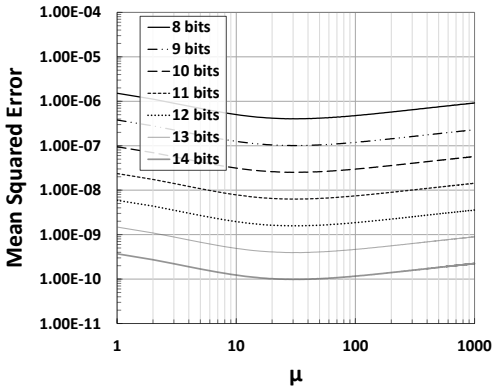

(b) Mean Squared Error for the μ-law quantization varying μ

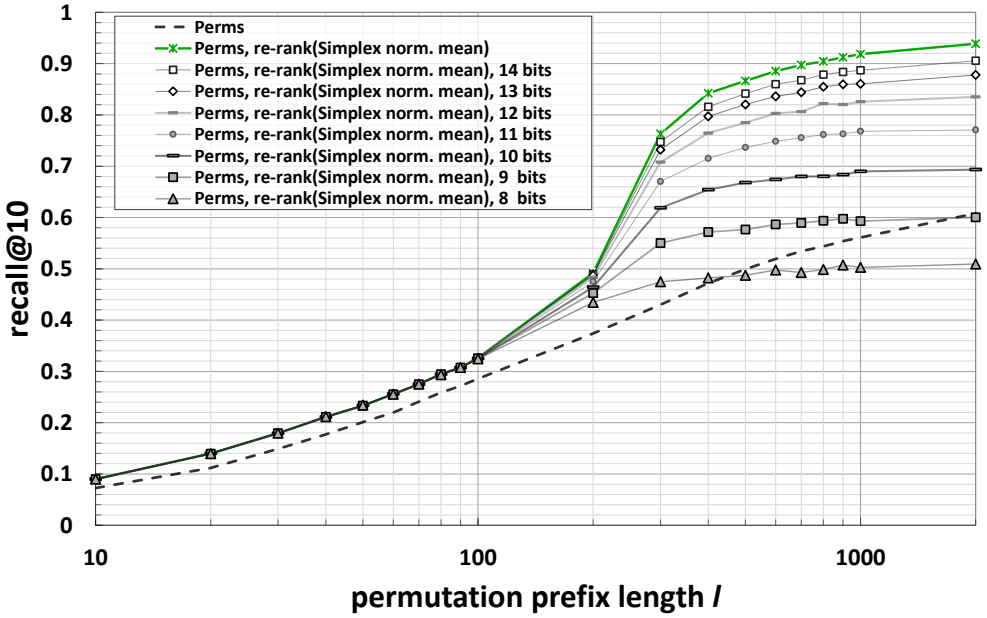

(c) *Recall*@10 varying the permutation prefix length l ($\mu = 40$)

Figure 14: *Twitter Glove, Cosine distance,* $n = 4,000$

References

[1] P. Zezula, G. Amato, V. Dohnal, M. Batko, Similarity search: the metric space approach, Vol. 32, Springer Science & Business Media, 2006.

[2] A. Esuli, Use of permutation prefixes for efficient and scalable approximate similarity search, Information Processing & Management 48 (5) (2012) 889–902. doi:10.1016/j.ipm.2010.11.011.

[3] M. Patella, P. Ciaccia, Approximate similarity search: A multi-faceted problem, Journal of Discrete Algorithms 7 (1) (2009) 36–48. doi:10.1016/j.jda.2008.09.014.

[4] R. Weber, H.-J. Schek, S. Blott, A quantitative analysis and performance study for similarity-search methods in high-dimensional spaces, in: Proceedings of 24rd International Conference on Very Large Data Bases (VLDB'98), Vol. 98, Morgan Kaufmann, 1998, pp. 194–205.

[5] B. Naidan, L. Boytsov, E. Nyberg, Permutation search methods are efficient, yet faster search is possible, Proceedings of the 41st International Conference on Very Large Data Bases (VLDB) 8 (12) (2015) 1618–1629. doi:10.14778/2824032.2824059.

[6] V. Pestov, Indexability, concentration, and vc theory, Journal of Discrete Algorithms 13 (2012) 2–18. doi:10.1016/j.jda.2011.10.002.

[7] H. Ferhatosmanoglu, E. Tuncel, D. Agrawal, A. El Abbadi, Approximate nearest neighbor searching in multimedia databases, in: Proceedings 17th International Conference on Data Engineering (ICDE 2001), IEEE Computer Society, 2001, pp. 503–511. doi:10.1109/ICDE.2001.914864.

[8] R. Connor, F. A. Cardillo, L. Vadicamo, F. Rabitti, Hilbert Exclusion: Improved metric search through finite isometric embeddings, ACM Transactions on Information Systems (TOIS) 35 (3) (2016) 17:1–17:27. doi:10.1145/3001583.

[9] R. Connor, L. Vadicamo, F. A. Cardillo, F. Rabitti, Supermetric search, Information Systems 80 (2019) 108–123. doi:10.1016/j.is.2018.01.002.

[10] R. Connor, L. Vadicamo, F. Rabitti, High-dimensional simplexes for supermetric search, in: Proceedings of 10th International Conference on Similarity Search and Applications (SISAP 2017), Lecture Notes in Computer Science, Springer International Publishing, 2017, pp. 96–109. doi:10.1007/978-3-319-68474-1_7.

[11] G. Amato, E. Chávez, R. Connor, F. Falchi, C. Gennaro, L. Vadicamo, Re-ranking permutation-based candidate sets with the n-Simplex projection, in: Proceedings of 10th International Conference on Similarity Search and Applications (SISAP 2018), Lecture Notes in Computer Science, Springer International Publishing, 2018, pp. 3–17. doi:10.1007/978-3-030-02224-2_1.

[12] G. Amato, P. Savino, Approximate similarity search in metric spaces using inverted files, in: Proceedings of 3rd International ICST Conference on Scalable Information Systems (INFOSCALE 2008), ICST / ACM, 2008, pp. 28:1–28:10. doi:10.4108/ICST.INFOSCALE2008.3486.

[13] E. Chávez, K. Figueroa, G. Navarro, Effective proximity retrieval by ordering permutations, IEEE Transactions on Pattern Analysis and Machine Intelligence 30 (9) (2008) 1647–1658. doi:10.1109/TPAMI.2007.70815.

[14] G. Amato, C. Gennaro, P. Savino, MI-File: Using inverted files for scalable approximate similarity search, Multimedia Tools and Applications (3) (2014) 1333–1362. doi:10.1007/s11042-012-1271-1.

[15] E. S. Tellez, E. Chávez, G. Navarro, Succinct nearest neighbor search, Information Systems 38 (7) (2013) 1019–1030. doi:10.1016/j.is.2012.06.005.

[16] D. Novak, P. Zezula, PPP-Codes for large-scale similarity searching 24 (2016) 61–87. doi:10.1007/978-3-662-49214-7_2.

[17] E. Chávez, M. Graff, G. Navarro, E. S. Téllez, Near neighbor searching with K nearest references, Information Systems 51 (2015) 43–61. doi:10.1016/j.is.2015.02.001.

[18] G. Amato, F. Falchi, F. Rabitti, L. Vadicamo, Some theoretical and experimental observations on permutation spaces and similarity search, in: Proceedings of 7th International Conference on Similarity Search and Applications (SISAP 2014), Lecture Notes in Computer Science, Springer International Publishing, 2014, pp. 37–49. doi:10.1007/978-3-319-11988-5_4.

[19] G. Amato, F. Falchi, C. Gennaro, L. Vadicamo, Deep Permutations: Deep convolutional neural networks and permutation-based indexing, in: Proceedings of 9th International Conference on Similarity Search and Applications (SISAP 2016), Lecture Notes in Computer Science, Springer International Publishing, 2016, pp. 93–106. doi:10.1007/978-3-319-46759-7_7.

[20] K. Figueroa, R. Paredes, N. Reyes, New permutation dissimilarity measures for proximity searching, in: Proceedings of 11th International Conference on Similarity Search and Applications (SISAP 2018), Lecture Notes in Computer Science, Springer International Publishing, 2018, pp. 122–133. doi:10.1007/978-3-030-02224-2_10.

[21] M. L. Micó, J. Oncina, E. Vidal, A new version of the nearest-neighbour approximating and eliminating search algorithm (AESA) with linear preprocessing time and memory requirements, Pattern Recognition Letters 15 (1) (1994) 9–17. doi:10.1016/0167-8655(94)90095-7.

[22] R. Connor, L. Vadicamo, F. A. Cardillo, F. Rabitti, Supermetric search with the four-point property, in: Proceedings

of 9th International Conference on Similarity Search and Applications (SISAP 2016), Lecture Notes in Computer Science, Springer International Publishing, 2016, pp. 51–64. doi:10.1007/978-3-319-46759-7_4.
[23] L. M. Blumenthal, Theory and applications of distance geometry, Clarendon Press, 1953.
[24] I. J. Schoenberg, Metric spaces and completely monotone functions, Annals of Mathematics 39 (4) (1938) 811–841.
[25] L. Vadicamo, R. Connor, F. Falchi, C. Gennaro, F. Rabitti, SPLX-Perm: A novel permutation-based representation for approximate metric search, in: Similarity Search and Applications, Springer International Publishing, 2019, pp. 40–48. doi:10.1007/978-3-030-32047-8_4.
[26] R. Fagin, R. Kumar, D. Sivakumar, Comparing top k lists, SIAM Journal on discrete mathematics 17 (1) (2003) 134–160.
[27] L. Vadicamo, Enhancing content-based image retrieval using aggregation of binary features, deep learning, and supermetric search, Ph.D. thesis, University of Pisa (2018).
URL https://etd.adm.unipi.it/theses/available/etd-04242018-161334/
[28] M. Deza, H. Maehara, Metric transforms and euclidean embeddings, Transactions of the American Mathematical Society 317 (2) (1990) 661–671. doi:10.1090/S0002-9947-1990-0974513-6.
[29] R. Connor, A. Dearle, L. Vadicamo, Modelling string structure in vector spaces, in: Proceedings of the 27th Italian Symposium on Advanced Database Systems (SEBD 2019), CEUR-WS.org, 2019.
URL http://ceur-ws.org/Vol-2400/paper-45.pdf
[30] B. Thomee, B. Elizalde, D. A. Shamma, K. Ni, G. Friedland, D. Poland, D. Borth, L.-J. Li, YFCC100M: The new data in multimedia research, Communications of the ACM 59 (2) (2016) 64–73. doi:10.1145/2812802.
[31] J. Pennington, R.Socher, C. D. Manning, GloVe: Global Vectors for Word Representation, in: Proceedings of the 2014 Conference on Empirical Methods in Natural Language Processing (EMNLP 2014), ACL, 2014, pp. 1532–1543.
URL http://www.aclweb.org/anthology/D14-1162
[32] K. Figueroa, G. Navarro, E. Chávez, Metric spaces library, www.sisap.org/library/manual.pdf (2007).
[33] G. Amato, F. Falchi, C. Gennaro, F. Rabitti, YFCC100M-HNfc6: a large-scale deep features benchmark for similarity search, in: Proceedings of 9th International Conference on Similarity Search and Applications (SISAP 2016), Lecture Notes in Computer Science, Springer International Publishing, 2016, pp. 196–209. doi:10.1007/978-3-319-46759-7_15.
[34] B. Zhou, A. Lapedriza, J. Xiao, A. Torralba, A. Oliva, Learning deep features for scene recognition using places database, in: Advances in Neural Information Processing Systems 27: Annual Conference on Neural Information Processing Systems 2014, Curran Associates, Inc., 2014, pp. 487–495.
[35] E. Chávez, G. Navarro, R. Baeza-Yates, J. L. Marroquín, Searching in metric spaces, ACM computing surveys (CSUR) 33 (3) (2001) 273–321. doi:10.1145/502807.502808.
[36] A. Babenko, V. S. Lempitsky, The inverted multi-index, IEEE transactions on pattern analysis and machine intelligence 37 (6) (2015) 1247–1260. doi:10.1109/TPAMI.2014.2361319.
URL https://doi.org/10.1109/TPAMI.2014.2361319